Thermal and Mechanical Studies of PVP/2-HEC Blend Films

[1]M.F.H. Abd El-kader, [2]M. Abu-Abdeen

[1]Biophysics Department, Faculty of Science, Cairo University, Giza,12613, Egypt.
[2]Physics Department, Faculty of Science, Cairo University, Giza,12613, Egypt.

Abstract: Solid polymer blend films based on polyvinyl pyrrolidone (PVP) and 2-hydroxyethyl cellulose (2-HEC) were prepared in various concentrations by solution cast technique. X-ray diffraction, differential scanning calorimetry (DSC), thermogravimetric analysis (TGA), and stress-strain of individual polymers and their blended samples were studied. X-ray diffraction patterns demonstrate miscibility between the PVP and 2-HEC in amorphous region for blend system. DSC characterization on PVP/2-HEC blends revealed a single T_g in each composition and its position was slightly shifted towards higher temperatures with increasing PVP content, which further supports single-phase behavior. It was found from TGA and its derivatives that the mass loss of most samples is accomplished in two decomposition stages in the temperature range of investigation, indicating different degradation mechanisms. Making use of Coats-Redfern relation, TG data allowed the calculation of some thermodynamic parameters such as activation energy, entropy, enthalpy and Gibb's free energy. Stress-strain data indicated that the blends became more brittle as PVP content increased. The elastic modulus was found to increase as the amount of PVP increased, while the strain at break decreased in an opposite behavior. Meanwhile, the tensile strength had a maximum value at 30 wt % PVP content in blend samples.

Key words: polymers; differential scanning calorimetry (DSC); thermogravimetric analysis (TGA); mechanical testing.

INTRODUCTION

Polymer blends are very important and belong to a rapidly advancing branch in polymer science and technology because of their widely used applications as bioequivalent materials [Garrel *et al.* (1991); Chuang *et al.* (1999)]. The miscibility between the constituents of a polymer mixture is an important factor in the development of new materials based on polymeric blends [Wanchoo and Sharma (2003); Abd El-kader *et al.* (2010) and Abd El-kader *et al.* (2013)]. Blend films may be designed to take advantages of the characteristics of the pure components, which should be chemically compatible, to enhance thermal and mechanical properties of the new biofilms.

Polyvinyl pyrrolidone is very useful in pharmacy and medicine because of its outstanding absorption and complex abilities. It is also, used for the preparation of synthetic plasmas as well as to creations of hydrogels and thromboresistent hydrophilic gels [Rosiak *et al.* (1987); Ciardelli *et al.* (2002) and Eisa *et al.* (2012)]. Cellulose is the most abundant polysaccharides, and occurs mainly within the cell wall of higher plants as a structural material, which is water-insoluble [Coffey *et al.* (1995)]. Substitution of hydroxyl groups within the cellulose backbone by some functional groups provides cellulose with water-solubility through the decrease in the crystallinity of the molecule. Hydroxyethyl cellulose is a gelling and thickening agent derived from cellulose [Dai *et al.* (1998)]. It is widely used with hydrophobic drugs in capsule formulations, to improve the drug dissolution in the gastrointestinal fluids [Ivarsson and Wahlgren (2012)]. Other applications include control of emulsion stability in hair conditioning and used for viscosity modification in paints and cosmetics [Patruyo *et al.* (2002)]. A detailed literature survey suggested that no information is available on PVP/2-HEC blends. Both PVP and 2-HEC are water-soluble. Accordingly, the blend of PVP and 2-HEC may give the possibility of producing a new material for potential biomedical applications.

The aim of this work is to perform a study on the effect of composition ratio on thermal and mechanical properties of PVP/2-HEC (wt/wt %) blends. Attention has been paid to discuss some thermodynamic parameters and elastic behavior related to the investigated samples.

Experimental:
Both PVP and 2-HEC of molecular weights 40,000 and 250,000, respectively, were supplied by Sigma-Aldrich, USA. Weighed amounts of PVP and 2-HEC were dissolved in distilled water at room temperature. Solutions of both PVP and 2-HEC were mixed together by the weight percentages 85/15, 70/30, 50/50, 30/70 and 15/85 (wt/wt %) PVP/2-HEC with a magnetic stirrer at 50 °C. Thin films of these blends were cast onto

---

Corresponding Author: M. F. H. Abd El-kader, Biophysics Department Faculty of Science, Cairo University, Giza,12613, Egypt.
E-mail: mfhamed@hotmail.com,   phone: +2(02)33468923

stainless steel Petri-dishes and then dried at room temperature for six days until the solvent was completely evaporated.

X-ray diffraction (XRD) patterns were obtained with XRD (Scintag) by cu k_α radiation (Cupertino, CA). Thermal analysis of the prepared blend films was carried out with computerized differential scanning calorimeter (DSC) and thermogravimetric analysis (TGA) instruments (TA-50) by Shimadzu Carp (Kyoto, Japan). Analysis was done under an atmospheric of nitrogen at a flow rate of 30 ml/min. The heating rate used for all of the samples under investigation was 10 °C/min. Stress-strain tests were carried out on a DMA Q800 machine TA instruments (USA), using the tension film clamping arrangement at a force rate of 0.5 N/min. Specimens in the form of filmstrips with dimensions 15 mm length, 4 mm width and 0.1 mm thick were used.

RESULT AND DISCUSSION

X-ray Diffraction (XRD):

Typical XRD patterns of both PVP and 2-HEC homopolymers and their blend sample of composition 50/50 (wt/wt %) at room temperature are shown in Fig. 1. XRD patterns of all samples reveal no Bragg diffractions. The x-ray spectrum of pure PVP film exhibited an amorphous feature characterized by two halos centered at 2θ = 11.5° and 22.5°, which is in agreement with published data [Razzak *et al.* (1999); Liu *et al.* (2004) and Abo-Talb (2009)]. Also, the x-ray spectrum of pure 2-HEC shows an amorphous halo with scattered intensity maximum corresponding to $2\theta = 22°$.
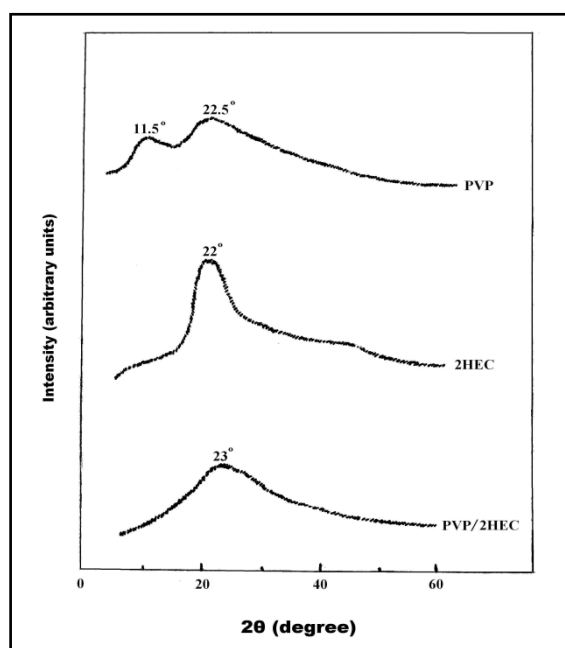

Fig. 1: X-ray diffraction patterns for PVP and 2-HEC homopolymers and blend sample of composition 50/50 (wt/wt %).

In case of x-ray spectrum of blend sample shows a broad halo amorphous larger than that found in individual polymers, which is centered at $2\theta = 23°$. It is known that glassy amorphous polymers are typically clear; they show a liquid-like x-ray pattern [Wignall (1993)]. This is consistent with results of the investigated samples. Thus, the x-ray diffraction spectra indicate that the miscibility between the amorphous components of both homopolymers is possible.

Thermal Properties:
Differential Scanning Calorometry:

Differential scanning calorimetry is a convenient tool to determine the physical and chemical changes such as glass transition temperature (T_g), melting point (T_m) and thermal decomposition temperature (T_d). Fig. 2 shows the DSC thermograms for PVP and 2-HEC homopolymers as well as their blends in the temperature range 30 – 400 °C. DSC curve of PVP shows two-phase transitions, the first is related to the water bonded to molecules at 74 °C and the second corresponds to a glass transition temperature at 130 °C. In addition, the melting phase transition for PVP could not be observed in the measured temperature range of DSC scan. This may be a direct result of the rigid nature of PVP molecular backbones. It is reported in the literature [Blecher *et*

al. (1980); Kuo *et al.* (2002) and Sionkowska (2003)] that the value of T_g varied in the range 86 – 178 ^{o}C. In the present study, the value of T_g is in agreement with that found by Kuo *et al.* (2002). This variation of T_g values is attributed to the difference in molecular weight and the preparation conditions of PVP films. In case of pure 2-HEC, two endothermic peaks appeared at 66 and 270 ^{o}C corresponding to glass transition and melting point, respectively. These values are nearly in agreement with that previously reported [Marianiova *et al.* (1992)].
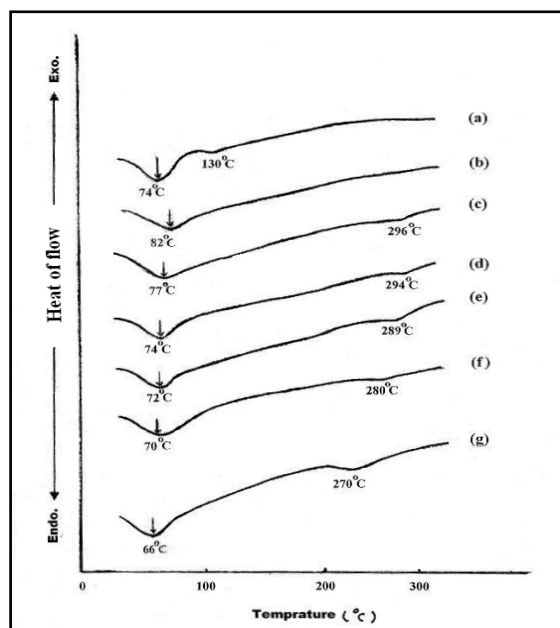

Fig. 2: DSC thermograms for PVP/2-HEC blend samples; (a) 100/0, (b) 85/15, (c) 70/30, (d) 50/50, (e) 30/70, (f) 15/85 and (g) 0/100 (wt/wt %).

It was of particular interest to estimate how the thermal transition of blend samples varied after mixing with different concentrations. It is generally accepted that the presence of two separate T_g's in blend polymers provides a strong signature of immiscibility. However, miscible blends could exhibit a broadened T_g that could be related to a disparity in the blend component mobility, concentration fluctuations, or both. Amorphous/amorphous blends can be produced in which the glass transition process is controlled in terms of peak temperature, width, and amplitude [Cheung and Guest (2000)]. It is clear from DSC curves from (b) to (f) in Fig. 2 that the blends with different composition ratio can be considered miscible, as indicated by the presence of a single T_g in-between the T_g's of the pure polymers. The transition width of the T_g for the blends is almost identical to those of pure components, which further supports single-phase behavior in the blends. Besides, the melting point of 2-HEC shifted towards higher temperatures with increasing PVP content in blend samples but with decreasing intensities and become faint. Since pyrrolidone rings in PVP contain a proton accepting carbonyl groups, while 2-HEC contain CH_2OR groups, where R=H or $(CH_2CH_2O)_n$-H and ethylene oxide groups substituted on hydroxyl groups in the glucosidic bond, so we can expect some interactions between these two macromolecules. Thus, the blends formed from PVP and 2-HEC have been shown to be miscible due to the presence of groups capable of hydrogen bonding.

Thermogravimetric Analysis:
The thermogravimetric analysis curves of PVP and 2-HEC pure polymers and their blends are indicated in Fig. 3. It can be seen from the Figure that all samples present two stages of decomposition in mass loss curves except the blend sample containing 30 wt % PVP has three stages of decomposition. The first step from room temperature up to approximately 190 ^{o}C represents the evaporation of residual absorbed water.

The second step starts at approximately 216 ^{o}C and ends at about 400 ^{o}C, which included melting point of 2-HEC and its degradation temperature. Table 1 represents the decomposition steps and percentage weight loss for individual polymers and their blends. The presence of more weight loss in the second decomposition region for pure 2-HEC than both pure PVP and blend samples suggests that it has a lower thermal stability (see Table 1). Also, it is clear from Table 1 that the blend sample of 30 wt % PVP content has a lower total weight loss than other samples indicating that there are intermolecular crosslinking reactions have a stabilizing thermal effect.
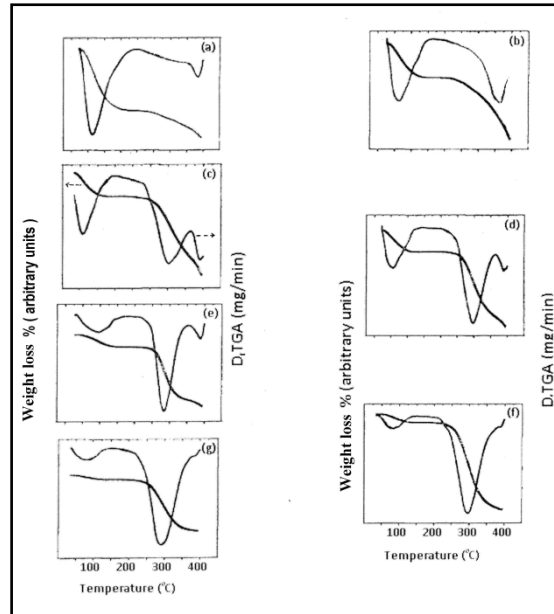
Fig. 3: TGA and DrTGA for PVP/2-HEC blend samples; (a) 100/0, (b) 85/15, (c) 70/30, (d) 50/50, (e) 30/70, (f) 15/85 and (g) 0/100 (wt/wt %).

Table 1: TG and DrTG data for PVP/2-HEC (wt/wt %) blend samples.

PVP/2-HEC (wt/wt %)	Steps	Temperature range (°C)	DrTGA T_p (°C)	Weight loss %	
				Partial	Total
100/0	1st	21 – 190	62	11.07	16.21
	2nd	229 - 399	383	5.14	
85/15	1st	26 – 146	62	10.06	29.98
	2nd	226 – 397	330	19.92	
70/30	1st	32 – 106	59	7.76	30.36
	2nd	228 – 364	302	22.60	
50/50	1st	21 – 119	55	11.10	36.82
	2nd	245 – 362	297	35.72	
30/70	1st	31 – 138	89	10.47	15.26
	2nd	238 – 348	284	2.81	
	3rd	355 – 397	387	1.98	
15/85	1st	36 – 120	81	4.79	40.34
	2nd	218 – 380	296	35.55	
0/100	1st	34 – 125	79	5.35	72.39
	2nd	216 – 380	290	67.04	

The difference in the thermal decomposition behavior of different samples can be seen more clearly from the derivative thermogravimetric (D_rTG) curves shown in Fig. 3. The D_rTG curves for all samples show two broad peak temperatures T_p's corresponding to regions I and II except the blend sample contain 30 wt % PVP which has an additional narrow peak corresponding to region III. This T_p was used as a measure of thermal stability. The relevant data are summarized in Table 1. The data revealed that the thermal stability of the blend sample of 30 wt % PVP has a higher thermal stability compared to other blends as indicated by the higher T_p value of 89 °C in first decomposition step. This result is consistent with the presented total weight loss data.

Thermodynamic activation parameters of decomposition process were evaluated by making use of the well-known Coats-Redfern relation [Coats and Redfern (1964); Fernands *et al.* (2001) and Chiang *et al.* (2002)], non-isothermal kinetic method in the following form:

for n≠1

$$\ln\left[\frac{1-(1-\alpha)^{1-n}}{T^2(1-n)}\right] = \ln\frac{AR}{\beta E}\left(1 - \frac{2RT}{E}\right) - \frac{E}{RT} \tag{1}$$

for n=1

$$\ln\left[\frac{-\ln(1-\alpha)}{T^2}\right] = \ln\frac{AR}{\beta E}\left(1 - \frac{2RT}{E}\right) - \frac{E}{RT} \tag{2}$$

where *A* is a constant, β is the heating rate, *R* is the universal gas constant, *E* is the activation energy, n is the order of reaction and α is the fractional weight loss. The best value of n is found to be nearly equal one using

trial method, where the fitting to the experimental data is satisfactory for two stages of decomposition. The plots of $ln\left[\frac{-ln(1-\alpha)}{T^2}\right]$ against $\frac{1}{T}$ for all samples in decomposition steps give straight lines as shown in Figs. 4 and 5. The slopes of these lines give $\frac{E}{R}$, so the activation energy E can be calculated.
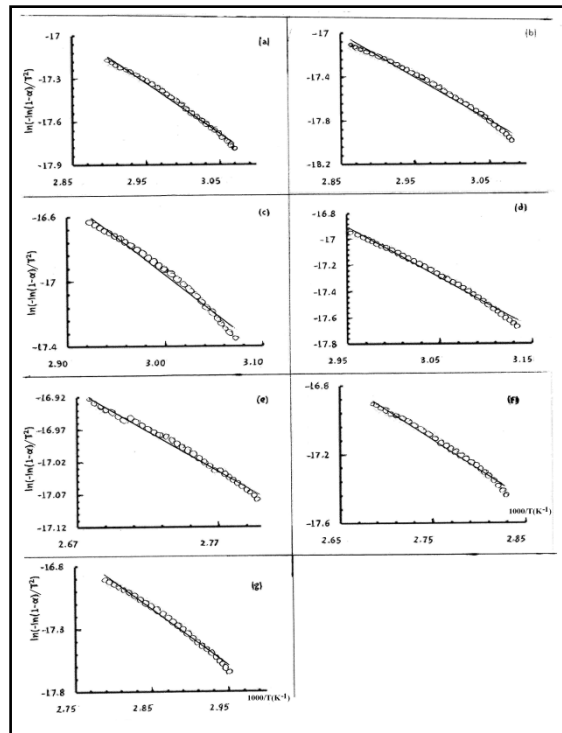

Fig. 4: Coats-Redfern plots of the first decomposition step for PVP/2-HEC blend samples; (a) 100/0, (b) 85/15, (c) 70/30, (d) 50/50, (e) 30/70, (f) 15/85 and (g) 0/100 (wt/wt %).
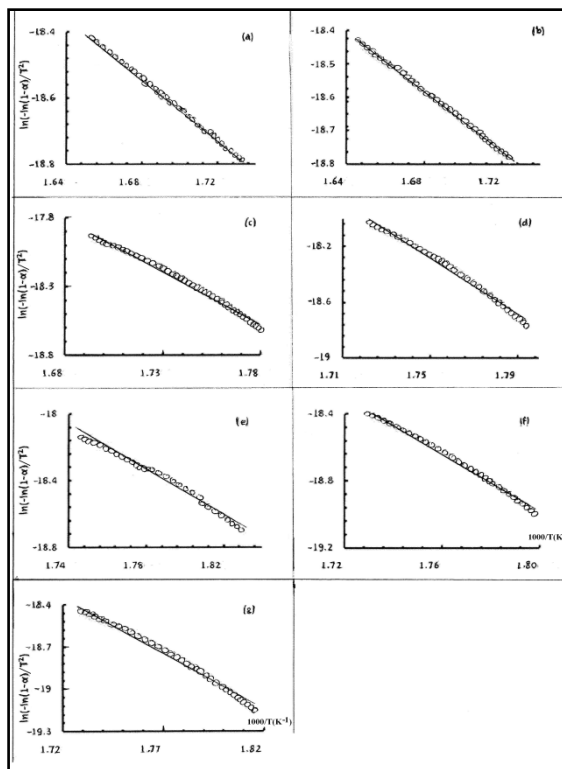

Fig. 5: Coats-Redfern plots of the second decomposition step for PVP/2-HEC blend samples; (a) 100/0, (b) 85/15, (c) 70/30, (d) 50/50, (e) 30/70, (f) 15/85 and (g) 0/100 (wt/wt %).

The activation entropy (ΔS^*), the activation enthalpy (ΔH^*) and the Gibb's free energy of activation (ΔG^*) are calculated using the following equations [Yakuphanoglu *et al.* (2004)]

$$\Delta S^* = 2.3031 \log\left(\frac{Ah}{K_B T_P}\right) R \tag{3}$$

$$\Delta H^* = E - RT_P \tag{4}$$

$$\Delta G^* = \Delta H^* - T_P \Delta S^* \tag{5}$$

where K_B and h are Boltzmann and Planck constants, respectively and T_p is the D_rTG peak temperature. The calculated values of E, A, ΔS^*, ΔH^* and ΔG^* for the first and second decomposition steps are given in table 2. The data obtained in the first decomposition step indicate that the blend sample of 30 wt % PVP content has more thermal stability, more order and less total thermal motion compared to other samples. Also, the blend sample 70 wt % PVP content has less order than the other samples. In the second decomposition step, the blend sample 85 wt % PVP content has a more thermal stability and less total thermal motion compared to other samples. Also, the blend sample of 50 wt % has a less order than the other samples. The values of E, ΔH^* and ΔG^* in the first decomposition step are lower than the values of the second decomposition step. This result indicates that the nature of the first decomposition region is of low total thermal motion and more thermal stability with respect to the second decomposition region. The initial lower E value is likely associated with initiation process that occur at weak links of PVP and 2-HEC, which is, however, a limited step of degradation. By increasing the temperature, random scission of macromolecular chains predominates and the activation energy has a greater value. Besides, all the samples have negative entropy, which indicates ordered systems and more ordered activated states that may be possible through the chemosorption of other light decomposition products.

Table 2: Thermodynamic parameters of the thermal decomposition steps of PVP/2-HEC (wt/wt %) blend samples.

PVP/2HEC (wt/wt %)	stage	Thermodynamic Parameters				
		E (J mol^{-1})	A (s^{-1})	ΔS^* (J mol^{-1} K^{-1})	ΔH^* (J mol^{-1})	ΔG^* (J mol^{-1})
100/0	1st	2.95×10^4	1.8×10^1	-222.1	2.67×10^4	2.39×10^4
	2nd	3.84×10^4	4.5×10^{-1}	-257.3	3.35×10^4	2.85×10^4
85/15	1st	3.27×10^4	5.6×10^1	-212.4	2.99×10^4	2.71×10^4
	2nd	3.75×10^4	3.5×10^{-1}	-259.3	3.26×10^4	2.76×10^4
70/30	1st	3.90×10^4	1.2×10^3	-186.7	3.62×10^4	3.34×10^4
	2nd	6.33×10^4	2.4×10^2	-205.0	5.85×10^4	5.37×10^4
50/50	1st	3.25×10^4	8.6×10^1	-209.5	2.95×10^4	2.65×10^4
	2nd	8.39×10^4	2.5×10^4	-166.0	7.91×10^4	7.44×10^4
30/70	1st	1.04×10^4	7.7×10^3	-287.0	7.01×10^3	4.38×10^3
	2nd	5.68×10^4	6.8×10^1	-215.1	5.22×10^4	4.75×10^4
15/85	1st	2.93×10^4	9.9×10^0	-227.5	2.63×10^4	2.33×10^4
	2nd	7.12×10^4	1.1×10^3	-191.9	6.64×10^4	6.17×10^4
0/100	1st	3.76×10^4	3.0×10^3	-198.7	3.47×10^4	3.18×10^4
	2nd	6.70×10^4	3.4×10^2	-201.8	6.13×10^4	5.66×10^4

Mechanical Properties:

The stress-strain curves of pure 2-HEC and the blend samples of compositions 85/15, 70/30, 50/50, 30/70 and 15/85 PVP/2-HEC (wt/wt %) are illustrated in Fig. 6. The pure PVP sample is brittle and it is hard to deal with it and so it was not tested. Initially a viscoelastic response that is considered to be fully reversible is found. For small stresses the blends behavior is linear viscoelastic, while with increasing stress the behavior becomes progressively nonlinear. At the yield point the deformation becomes irrecoverable since stress-induced plastic flow sets in leading to a structural evolution which reduces the material's resistance to plastic flow, strain softening.

The origin of the deformation of polymer materials lies in their ability to adjust their chain conformation on a molecular level by rotation around single covalent bonds in the main chain. This freedom of rotation is, however, controlled by intermolecular (chain stiffness) and intermolecular (inter-chain) interactions. Together these interactions give rise to an energy barrier that restricts conformational change(s) of the main chain [Bauwens-Crowet *et al.* (1969)]. As the applied stress exceeds this barrier, chain scission takes place resulting as a softening of the material. Yielding occurs when the polymer backbone chains begin to disentangle [Rubatat *et al.* (2004); Van Der Heijder *et al.* (2004) and Lui *et al.* (2006)]. As the amount of PVP content increased, the blend samples become more brittle as indicated from the behavior illustrated in Fig. 6.
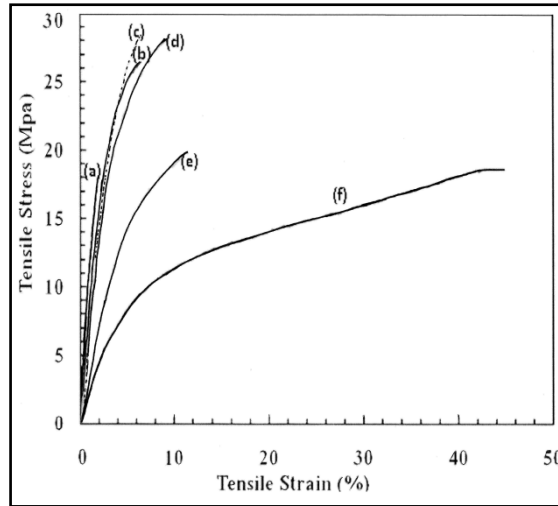
Fig. 6: Stress-strain curves at room temperature for PVP/2-HEC blend samples; (a) 100/0, (b) 85/15, (c) 70/30, (d) 50/50, (e) 30/70, (f) 15/85 and (g) 0/100 (wt/wt %).

Separate plots of the change of stress and strain $d\sigma/d\varepsilon$ versus strain ε are performed for all blend samples (figures not shown). It shows strain-independent regions at very low strain values. These constant values are taken to be the elastic modulus (E_{el}) for the different compositions, which are shown in Fig. 7. The addition of PVP to 2-HEC increases the elastic modulus from 0.23 GPa for pure 2-HEC to 1.77 GPa for blend sample of 85 wt % PVP content.
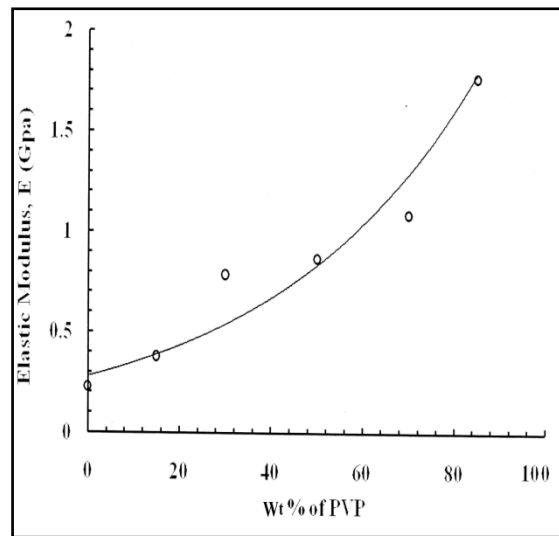

Fig. 7: The elastic modulus of PVP/2-HEC blends at room temperature.

Tensile strength σ_b and strain at break ε_b of the samples under investigation are shown in Fig. 8. It is clear from the Figure that ε_b decreases with increasing PVP content in the blend samples. It must be also mentioned that the strain at break has an opposite behavior to that of the elastic modulus. Tensile strength, on the other hand, increases with increasing PVP content and reaches a maximum value of 28.4 MPa for blend sample of 30 wt % PVP and then followed by a decrease up to 85 wt %. The chains of 2-HEC are easily moved and oriented in the direction of the applied stress making this polymer more flexible, while the chains of PVP are hard to reorient themselves parallel to the applied stress making it more brittle. Chains of PVP restrict the motion of the chains of 2-HEC on blending them which results in the increase of the elastic modulus and a decrease in the strain at break. Besides, for PVP concentrations less than or equal to 30 wt % the tensile strength increases due to some sort of interaction between the hard PVP phase and the host 2-HEC. Further increase of PVP (greater

than 30 wt %) in blend samples, the hard phase predominates and may make aggregates which results in less interaction with the soft one (2-HEC). This leads to a decrease in the tensile strength.
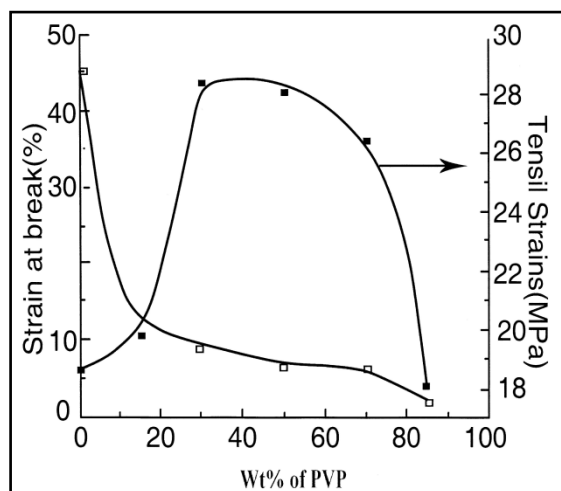

Fig. 8: The strain at break and the tensile strength of PVP/2-HEC blends at room temperature.

Conclusion:

The results obtained from this work demonstrate that blending PVP with 2-HEC causes considerable changes in the structure, thermal and mechanical characterizations of the resultant polymeric system. X-ray diffraction, DSC and mechanical data indicate that the blends of PVP and 2-HEC are miscible due to the presence of polar groups capable of interacting through hydrogen bond, which gives a compatible impact blends. However, TG and D_rTG thermograms show that the thermal stability of 2-HEC in the first decomposition step is enhanced by the addition of PVP up to 30 wt %. This result was confirmed from Gibb's free energy data. Also, the blend sample containing 30 wt % PVP had a maximum value of tensile strength. These properties obtained for 30 wt % PVP content blend sample prefer its use in a board scope for many medical and industrial applications. Therefore, it is recommended to take into consideration the role of additive concentration of chemical compounds in obtaining polymeric materials with specific characterization.

REFERENCES

Abd El-Kader, F.H., S.A. Gafer, A.F. Basha, S.I. Bannan, M.A.F. Basha, 2010. Thermal and optical properties of gelatin/poly(vinyl alcohol) blends. J Appl Polym Sci., 118: 413-420.

Abd El-Kader, F.H., W.H. Osman, R.S. Hafez, 2013. DC conduction mechanism and dielectric properties of poly(methyl methacrylate)/Poly(vinyl acetate) blends doped and undoped with malachite green. Physica B., 408: 140-150.

Abo-Talb, M.H., 2009. Thermal and spectroscopic studies of poly(N-vinyl pyrrolidone)/poly(vinyl alcohol) blend films. J Appl Polym Sci., 114: 1202-1207.

Bauwens-Crowet, C., J.C. Bauwens, G. Homès, 1969. Tensile yield-stress behavior of glassy polymers. J Polym Sci Part A-2: Polymer Physics, 7: 735-742.

Blecher, L., D.H. Lorenz, H.L. Lowd, A.S. Wood, D.P. Wyman, 1980. Polyvinylpyrrolidone. In: Davidson RL (ed) Handbook of Water-soluble Gums and Resins, McGraw-Hill Book Company, New York, NY, pp: 1-21.

Cheung, Y.W., M.J. Guest, 2000. A study of the blending of ethylene-styrene copolymers differing in the copolymer styrene content: Miscibility considerations. J Polym Sci Part B: Polym Phys., 38: 2976-2987.

Chiang, C.L., F.Y. Wang, C.C.M. Ma, H.R. Chang, 2002. Flame retardance and thermal degradation of new epoxy containing silicon and phosphorous hybrid creamers prepared by the sol-gel method. Polymer Degradation and Stability, 77: 273-278.

Chuang, W.Y., T.H. Young, C.H. Yao, W.Y. Chiu, 1999. Properties of the poly(vinyl alcohol)/chitosan blend and its effect on the culture of fibroblast in vitro. Biomaterials, 20: 1479-1487.

Ciardelli, G., C. Cristallini, N. Barbani, G. Benedetti, A. Crociani, L. Travison, *et al.*, 2002. Bioartificial polymeric materials: α-amylase, poly(2-hydroxyethyl methacrylate), poly(N-vinylpyrrolidone) system. Macromol Chem Phys., 203: 1666-1673.

Coats, A.W., J.P. Redfern, 1964. Kinetic parameters from thermogravimetric data. Nature, 201: 68-69.

Coffey, D.G., D.A. Bell, A. Henderson, 1995. Food polysaccharides and their applications. Morcel Dekker Inc, NewYork, pp: 123-153.

Dai, Q., J. Chen, Y. Huang, 1998. Toughening of epoxy resin blended with thermotropic hydroxyethyl cellulose acetate. J Appl polym Sci., 70: 1159-1163.

Eisa, W.H., Y.K. Abdel-Moneam, A.A. Shabaka, A.M. Hosam, 2012. In situ approach induced growth of highly monodispersed Ag nanoparticles within free standing PVA/PVP films. Spectrochemica acta, A95: 341-346.

Fernandes, V.J., A.S. Araujo, G.J.T. Fernandes, J.R. Matos, M. Ionashiro, 2001. Kinetic parameters of polymer degradation by SAPO-37. Journal of Thermal Analysis and Colorimetry, 64: 585-589.

Garrel, D.R., P. Gaudreau, L. Zhang, *et al.*, 1991. Chronic administration of growth hormone-releasing factor increases wound strength and collagen maturation in granulation tissue. J Surg Res., 51: 279-302.

Ivarsson, D., M. Wahlgren, 2012. Comparison of in vitro methods of measuring mucoadhesion: Ellipsometry, tensile strength and rheological measurements. Colloids and surfaces, B92: 353-359.

Kuo, S.W., S.C. Chan, F.C. Chang, 2002. Miscibility enhancement on the immiscible binary blend of poly(vinyl acetate) and poly(vinyl pyrrolidone) with bisphenol A. Polym., 43: 3653-3660.

Liu, H.G., Y. Lee, W.P. Qin, K. Jang, X.S. Feng, 2004. Studies on composites formed by europium complexes with different ligands and polyvinylpyrrolidone. Mater Lett., 58: 1677-1682.

Lui, D., S. Kyriakides, S.W. Case, J.J. Lesko, Y. Li, J.E. Mcgrath, 2006. Tensile behavior of Nafion and sulfonated poly(arylene ether sulfone) copolymer membranes and its morphological correlation. J Polym Sci Part B: Polymer Physics, 44: 1453-1465.

Marianiova, D., L. Lapcik, M. Pisarcik, 1992. Study of electrical properties of cellulose derivatives. Acta Polymerica, 43: 303-306.

Patruyo, L.G., A.J. Muller, A.E. Saez, 2002. Shear and extensional rheology of solutions of modified hydroxyethyl cellulose and sodium dodecyl sulfate. Polym., 43: 6481-6493.

Razzak, M.T., Zainuddin, Erizal, S.P. Dewi, *et al.,* 1999. Radiat Phys Chem., 55: 153-165.

Rosiak, J.J., K.K. Burczak, J.J. Olejniczak, W.W. Pekala, 1987. Polymer materials for biomedical purposes obtained by radiological methods. Polim Med., 17: 99-116.

Rubatat, L., G. Gebel, O. Diat, 2004. Fibrillar structure of Nafion: matching Fourier and real space studies of corresponding films and solution. Macromolecules, 37: 7772-7783.

Sionkowska, A., 2003. Interaction of collagen and poly(vinyl pyrrolidone) in blends. Europ Polym J., 39: 2135-2140.

Van Der Heijden, P.C., L. Rubatat, O. Diat, 2004. Orientation of drawn Nafion at molecular and mesoscopic scales. Macromolecules, 37: 5327-5336.

Wanchoo, R.K., P.K. Sharma, 2003. Viscometric Study on the compatibility of some water soluble polymer-polymer mixtures. Euro Polym J., 39: 1481-1482.

Wignall, C.D., 1993. Scattering technique in physical properties of polymers. In: Mard JE (ed) 2nd edn., American Chemical Society, Washington DC.

Yakuphanoglu, F., A.O. Gorgulu, A. Cukurovali, 2004. An organic semiconductor and conduction mechanism: N-[5-methyl-1,3,4-tiyodiazole-2-y] ditiyocarbamate compound. Physica, B353: 223-229.